Electron velocity distribution function at low electron densities in the positive column of a helium gas discharge

M.V. Chegotov*
Institute of Experimental Physics V, Ruhr-University Bochum, D-44780, Federal Republic of Germany
(Received 26 January 1994)

The electron velocity distribution function (EVDF) in the positive column of a helium gas discharge is derived taking into account both the spatial electron diffusion as an electron loss and associative ionization (AI) as an electron source. The latter is introduced into the kinetic equation for the EVDF and takes into account the typical features of the energy spectrum of electrons ejected during AI, i.e., the energetic structure of the electron source. The derived distribution function permits one to avoid the otherwise very essential discrepancy between theory and experiment, featuring agreement even in the fine details.

PACS number(s): 52.90.+z

INTRODUCTION

The interest in investigating gas discharges at low electron densities has several reasons. For example, one of these is the interest in the electromagnetic properties of atmosphere and ionosphere [1–3]. Of course, these is also great interest in such plasmas because of their broad use in industry and research and, in particular, because they can provide fundamental data on basic processes necessary for such applications. In order to investigate the energetic structures of electron sources in the energy spectrum one should deal with as small a number of these sources as possible. Aiming at these investigations, both for theory and experiment it is essential to go to as low electron densities as feasible.

It is obvious from the physical point of view that the larger the electron swarm mean energy $\bar{\epsilon}$ the larger is the probability to open new channels of free electron creation. In particular, the direct inelastic electron collision (DI) and stepwise inelastic electron collision (SI) ionizations assume a significant role at comparatively large magnitudes of the heating reduced electric field $E/N \geq 2.5 \times 10^{-16}$ V cm^2, where N is the density of neutral species [4]. Thus, keeping in mind the necessity of reducing the number of such electron sources in the energy spectrum one has also to choose plasma conditions of lower reduced electric field.

One of those experiments, with the positive column of a helium glow discharge at room gas temperature, which was carried out at low electron densities $n_e \sim 10^{10}$–10^{11} cm^{-3} in helium at pressure p of about several Torr and not large magnitudes of the electric field E ($E/N < 7 \times 10^{-17}$ V cm^2), is the experiment [5]. One of the most important advantages of this experiment is an application of the Thomson scattering technique to electron velocity distribution function (EVDF) measurements, which means that the influence of the measuring tools on the gas discharge was reduced practically to zero as compared to Langmuir-probe measurements of EVDF. Besides that, the Langmuir-probe measurements are very questionable at such small electron densities and comparatively large gas pressure, since the electron Debye radius becomes less than the ion mean free path and comparable to that of the electron.

The measurements of EVDF [5] on the axis of a positive column indicate substantial discrepancies between the theoretical pattern of such positive columns and the experimental data. One of those contradictions becoming obvious in [5] is the magnitude of the mean electron energy $\bar{\epsilon}^{\text{expt}}$ which appears to be considerably less than the value $\bar{\epsilon}^D$ predicted by the conventional theory. The measured value $\bar{\epsilon}^{\text{expt}}$ is about 1.3 eV while the measured magnitude of the electric field E inside the positive column gives a theoretical value $\bar{\epsilon}^D$ of 2.7 eV [5]. Since the gas temperature remained at room level and both $\bar{\epsilon}^{\text{expt}}$ and the density of electrons were comparatively small, one can neglect the inelastic energy losses of electrons during their collisions with excited helium atoms as compared with electron energy losses during their elastic collisions with all neutral species. At the comparatively small electron energy $\epsilon = mv^2/2 < 4$ eV (m is the electron mass) the electron mean free path for elastic collisions in helium does not depend on electron velocity v [6,7]. Just because of this the theoretical mean electron energy $\bar{\epsilon}^D$ mentioned above was calculated with the help of a Druyvesteyn EVDF [see (10) below] [5].

In the present article the positive column of a helium glow discharge is investigated theoretically at comparatively small electric field $E/N \leq 2.5 \times 10^{-16}$ V cm^2 and gas discharge pressure p of several Torr. Referring to the experiment [5] which manifests the small electron mean energy $\bar{\epsilon}$, we develop below a theory which explains such a small value of $\bar{\epsilon}$ not by inelastic collisions between electrons and neutral species but by the spatial diffusion and energetic structure of the free electron source in the gas discharge. It is shown that the most probable free electron source in the positive column at the experimental conditions of [5] is associative ionization [8,9]. This conclusion has strong support in particular in Ref. [4].

*Permanent address: P.N. Lebedev Physics Institute, Leninsky Prosp. 53, 117924 Moscow, GSP-1, Russia.

Nevertheless, in [4] the associative ionization (AI) is described as the free electron source in continuity equations only. This means that the energetic structure of this electron source is not resolved and is taken into account as an integral contribution to the electron swarm. In the present paper we take into account simultaneously the AI and its energetic structure as the free electron source and the spatial electron diffusion as the main electron loss. This enables us to come to an agreement with experiment [5] not only with respect to the magnitude of the mean electron energy but even with respect to the spectral shape of Thomson scattering. It should be noted that the theory developed below predicts a peculiarity of the EVDF in the region of $\bar{\epsilon}$ (see Fig. 1). The observation of such a peculiar structure could still be a subject for an experiment since it might have been that, because of the wide preference for the electron energy distribution function (EEDF), the effect was present in various measurements but could not be recognized. Because of the multiplication of the EVDF with $v \sim \sqrt{\epsilon}$ (see a definition of the EEDF, for example, in [10]) the EEDF always shows a peak at $\epsilon \neq 0$, and an additional contribution such as AI in the vicinity of this peak does not become so apparent as in the EVDF and a physical effect such as AI is blurred. It is for this effect that one should measure the EVDF rather than the EEDF. Just in connection with this task of discerning a broad spectral contribution to an otherwise monotically decreasing function, like the EVDF in most cases, attention should be drawn to an alternative regularization procedure [11] as an appropriate algorithm for the evaluation of Langmuir–probe and Thomson scattering measurements. This algorithm enables one to obtain just the EVDF from real experimental noisy data.

DISCUSSION OF FREE ELECTRON SOURCES

In this section we discuss the sources and patterns of free electron creation in a helium gas discharge under the above conditions. It is well known that the ionization potentials of helium atoms are comparatively large, whereby DI and SI are not so significant at comparatively small reduced electric fields $E/N \leq 2.5 \times 10^{-16}$ V cm^2 [4]. The experimental value appears to be sufficiently lower than this magnitude [5].

Under this condition the most important sources of free electrons in the positive column of a helium gas discharge are inelastic collisions between neutral species [8,9]. That is, the main candidates are the following two reactions: (1) the Penning reaction between all pairs of metastable species and He($2\,^3P$) states and (2) the reaction of AI between an excited helium atom He* and an atom in the ground state He($1\,^1S$):

$$\mathrm{He}^* + \mathrm{He}(1\,^1S) = \mathrm{He}_2{}^+ + e. \qquad (1)$$

As far as the experiment [5] is concerned, the gas discharge pressure p is comparatively low (about several Torr) and we can exclude the Penning reaction. Indeed, the optimum magnitude of gas pressure for the Penning

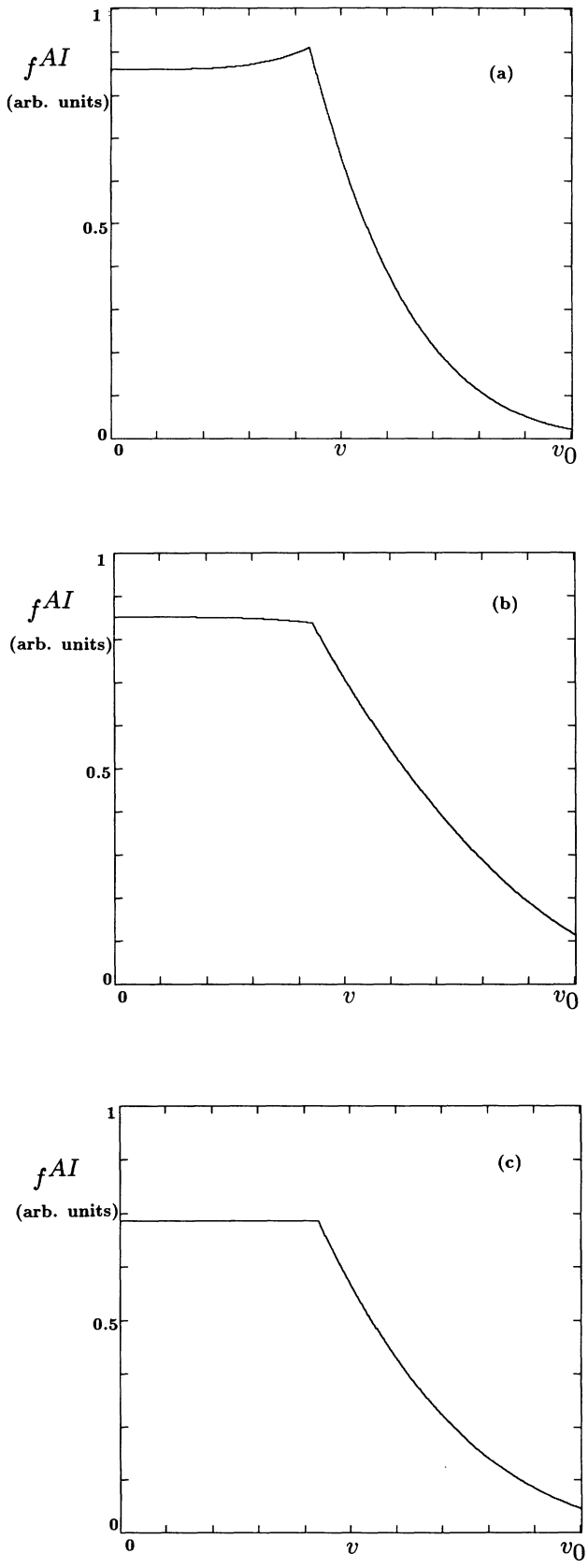

FIG. 1. The EVDF $f^{\mathrm{AI}}(v)$ in arbitrary units at different magnitudes of G: (a) $G = 2.7$, (b) $G = 0.5$, and (c) $G = 1$.

reaction ranges at higher $p \geq 15$ Torr (see, for example, [12]).

Thus, among the most probable ionization mechanisms one should discuss only one, namely, the associative ionization (1). The products of this reaction are a free electron and molecular ion He_2^+. The latter is rather stable, having a binding energy $\epsilon_{bi} = 2.23$ eV. In turn, this means that at present conditions the free positive charges in helium are molecular ions He_2^+. This conclusion finds its strong verification in experiments [13–15] carried out in a broad He pressure diapason. They discovered that the density of molecular ions He_2^+ was more than one order of magnitude larger than the density of atomic ions He^+. Nevertheless, in these experiments another reaction is considered as the molecular ion source. This is the so-called three-body ionic conversion [16]

$$He^+ + 2He(1\,^1S) = He_2^+ + He(1\,^1S). \quad (2)$$

Even if one neglects the facts that, first, it is impossible to exclude at all the reaction (1) as a probable source of He_2^+ in [13–15] and, secondly, the pressure in experiment [5] is lower than in [13–15] and so the probability of three-body reaction is lower than that of [13–15], the theoretical article [4] strongly confirms AI to be the dominant process of molecular ion creation. This is valid for not very strong reduced heating fields $E/N \leq 2.5 \times 10^{-16}$ V cm^2 and in the broad region of pressures 0.1 Torr $\leq p \leq 30$ Torr. In turn most of the free electrons are created by the AI (1) (see [4]).

The velocity distribution function of electrons produced by the AI has some peculiarities (see [17,18]) namely, the energies $\epsilon = \epsilon_{AI} + \delta\epsilon$ of electrons which are ejected during AI have very narrow dispersion $\delta\epsilon$. Here $\epsilon_{AI} = \epsilon_{bi} - \epsilon_{BE}$, where ϵ_{BE} is the binding energy of the electron in the excited atom He^*. From the point of view of electron energy scaling this leads to a bend of the EVDF at the point $v = v_{AI} = \sqrt{2\epsilon_{AI}/m}$, i.e., the first EVDF derivative with respect to velocity v jumps at the point $v = v_{AI}$. Further, we will show that in the experiment [5] the AI is in action under conditions which are far away from equilibrium. These conditions remove the EVDF from the equilibrium distribution. In particular, such a removal could be provided under nonstationary conditions. If the typical time of the nonstationarity τ_n sufficiently exceeds the time of EVDF relaxation to the equilibrium τ_r, the AI leads to a negligible bend of the EVDF at the point $v = v_{AI}$ and even the change in the slope of the EVDF is small compared to the typical slope in the vicinity of v_{AI} (see [18]). But if the conditions are far away from equilibrium, such as $\tau_n < \tau_r$, the EVDF is far from equilibrium, too, namely, the EVDF has a peak at the point $v = v_{AI}$ and the difference between EVDF derivatives from both sides of $v = v_{AI}$ is just equal to the EVDF derivative jump at $v = v_{AI}$ which was determined in [17].

Thus, in Ref. [18] the nonstationarity is the reason to drive the electron swarm far from equilibrium. In the present work another reason plays the same role. This reason is the spatial inhomogeneity of the positive column in the radial direction. Below, we will show that the spatial inhomogeneity leads the EVDF far away from equilibrium. This point of view is in accordance with the conventional assumption [19] that the electron losses in low pressure discharges are connected with spatial diffusion in the radial direction. In turn, as long as the electron mean energy $\bar{\epsilon}$ is comparatively small ($\bar{\epsilon} \leq 1.5$ eV) and the gas temperature remains at room value, the transport of the electrons in velocity space is guided by heating in the electric field E and cooling in elastic collisions with neutral species.

Thus we have in mind the following picture of EVDF formation which consists of two main elements. First, AI is the main distributed free electron source in the positive column and secondly transversal electron diffusion is the main electron loss. By the way, this picture is in strong agreement with the results of the numerical model [4]. An electron created by AI diffuses in space and, on one hand, loses energy in elastic collisions and, on the other hand, is gaining energy by acceleration in the electric field E.

SOLUTIONS OF THE KINETIC EQUATION

The kinetic equation, which describes the isotropic part of the EVDF $f(v)$ in the presence of AI, was proposed in Refs. [17,18]. At stationary conditions of inhomogeneous plasma this equation has the following form:

$$-\frac{v^2}{3\nu_e(v)}\Delta_r f - \frac{ev}{3\nu_e(v)m}\left\{\frac{\partial f}{\partial v}\mathrm{div}_r \mathbf{E} + (\mathbf{E}\nabla_r)\frac{\partial f}{\partial v}\right\} - \frac{e}{3mv^2}\frac{\partial}{\partial v}\left\{\frac{v^3}{\nu_e(v)}(\mathbf{E}\nabla_r)f\right\}$$

$$= \frac{1}{2v^2}\frac{\partial}{\partial v}\left[D(v)\frac{\partial f}{\partial v} + B(v)f\right] + \Delta S^{in}(f) + \frac{n_n^* \nu_{AI}}{4\pi v_{AI}^2}\delta(v - v_{AI}), \quad (3)$$

where $\Delta_r = (\nabla_r)^2 = \partial^2/\partial^2 x + \partial^2/\partial^2 y + \partial^2/\partial^2 z, \nabla_r = \mathbf{e}_x\partial/\partial x + \mathbf{e}_y\partial/\partial y + \mathbf{e}_z\partial/\partial z$ is the spatial gradient, $e = -|e|$ the electron charge, $\nu_e(v) = \nu_e^{el}(v) + \nu_e^{in}(v)$ the momentum transfer collision frequency between electrons and neutral species, and $\nu_e^{el}(v)$ [$\nu_e^{in}(v)$] is the elastic (inelastic) part of it.

$$D(v) = \frac{2e^2E^2v^2}{3m^2\nu_e(v)} + v^2 r_\Omega \frac{T_\Omega}{m},$$

where the last term in $D(v)$ describes in the general case the quantum electron energy loss of value $\hbar\Omega \ll mv^2/2$, T_Ω the effective temperature, and r_Ω the fraction of elec-

tron energy loss per second to excite the quantum of energy $\hbar\Omega$. $\Delta S^{\rm in}(f)$ takes into account the inelastic electron–neutral-species collisions with large electron energy change,

$$B(v) = \delta^{\rm el} v^3 \nu_e^{\rm el}(v) + r_\Omega v^3,$$

where $\delta^{\rm el} = 2m/M$ is the fraction of energy transferred from electron to neutral species at the electron–neutral-species elastic collisions and the δ–function term describes the AI source. n_n^* is the density of helium atoms with excited electrons at binding energy $\epsilon_{\rm BE} = \epsilon_{\rm bi} - mv_{\rm AI}^2/2$, $\mathbf{E}$ is the local electrical field in the discharge, and $\nu_{\rm AI}$ is the frequency of AI.

In the vicinity of the axis of the positive column, Eq. (3) takes the form

$$-\frac{v^2}{3\nu_e(v)}\Delta_r f = \frac{1}{2v^2}\frac{\partial}{\partial v}\left[D(v)\frac{\partial f}{\partial v} + B(v) f\right] + \frac{n_n^*\nu_{\rm AI}}{4\pi v_{\rm AI}^2}\delta(v - v_{\rm AI}). \quad (4)$$

Here we take into account that f depends only on the distance r from the axis, the radial component of the electric field $\mathbf{E}$ is small in the vicinity of the axis, and that the plasma is neutral there. The last assumption is justified by experimental work [20], where the radial component of $\mathbf{E}$ exibits a parabolic behavior as a function of r in the vicinity of the helium discharge axis. Also, we neglected $\Delta S^{\rm in}(f)$ since the mean electron kinetic energy $\bar{\epsilon}$ in the discharge of [5] is comparatively small ($\bar{\epsilon} \leq 1.5$ eV) and the gas temperature is equal to room temperature. Further, we neglect also the quantum energy losses r_Ω in $D(v)$ and $B(v)$ since the density of molecules He_2 is generally much smaller compared to the density of atomic helium [21]. These simplifications are completely in agreement with the above picture of the EVDF formation.

Then, at the point $r = 0$, we substitute $[-(a_0^2/R^2)f]$ for $\Delta_r f$. This substitution is obvious in the so-called Schottky-diffusion theory [22], where the density of electrons is proportional to the Bessel function $J_0(a_0 r/R)$, with R the tube radius, and where $a_0 \approx 2.405$ is the first zero of the Bessel function J_0. The results of the experimental EEDF measurements in the positive column cross section [20] state the possibility for a_0 to be several times larger than 2.405. Then the multiplication of (4) by $4\pi v^2$ and integration from 0 to v lead to the equation

$$\frac{\partial f}{\partial v} = \frac{1}{2\pi D(v)}\left\{\frac{4\pi}{3}\frac{a_0^2}{R^2}\int_0^v \frac{v'^4}{\nu_e(v')} f\, dv' - 2\pi B(v)\, f - n_n^*\nu_{\rm AI}\theta(v - v_{\rm AI})\right\}, \quad (5)$$

where $\theta(u)$ is the Heaviside step function and

$$\frac{4\pi}{3}\frac{a_0^2}{R^2}\int_0^\infty \frac{v^4}{\nu_e(v)} f\, dv = n_n^*\nu_{\rm AI}\,. \quad (6)$$

The last relation could be obtained from (5) by having v tend to infinity or from (4) in the more general form

$$-\frac{4\pi}{3}\int_0^\infty \frac{v^4}{\nu_e(v)}\Delta_r f\, dv = n_n^*\nu_{\rm AI},$$

which corresponds to the stationary continuity equation $\mathrm{div}_{\mathbf{r}}\mathbf{j} = n_n^*\nu_{\rm AI}$, where $\mathbf{j}$ is the electron flux. Taking into account that, first, the electron mean free path $l_e = v/\nu_e^{\rm el}(v)$ is independent of the velocity v at the electron energy $\epsilon = mv^2/2 \leq 4$ eV (see [6,7]), secondly, $\epsilon_{\rm AI} \leq 4$ eV, and, thirdly, nearly all electrons are at energies $\epsilon \leq 2$ eV, Eq. (5) takes the form

$$\frac{\partial f}{\partial v} = \frac{3m^2}{4\pi e^2 E^2 v l_e}\left\{\frac{4\pi}{3} l_e \frac{a_0^2}{R^2}\int_0^v v'^3 f\, dv' - 2\pi\delta^{\rm el} l_e^{-1} v^4 f - n_n^*\nu_{\rm AI}\theta(v - v_{\rm AI})\right\}. \quad (7)$$

The EVDF derivative $\partial f/\partial v$ is determined only by the diffusion $(4\pi/3) l_e (a_0^2/R^2)\int_0^v v'^3 f dv'$ and elastic collision $2\pi\delta^{\rm el} l_e^{-1} v^4 f$ terms in the velocity interval $(0, v_{\rm AI})$. For this interval it is convenient to rewrite Eq. (7) as

$$\frac{\partial f}{\partial v} + 4G v_0^{-4} v^{-1}\int_0^v v'^4 \frac{\partial f}{\partial v'} dv' = 4(G-1)\frac{v^3}{v_0^4} f, \quad (8)$$

where

$$G = (a_0^2/6)\left(\delta^{\rm el}\right)^{-1}(l_e/R)^2,$$

with $v_0 = [8e^2E^2 l_e^2/(3m^2\delta^{\rm el})]^{1/4}$. One can see from Eq. (8) that the sign of the EVDF derivative $\partial f/\partial v$ is guided by the sign of $G - 1$. That is, if the electron diffusion is comparatively fast, i.e.,

$$G > 1,$$

$\partial f/\partial v$ appears to be positive and $f(v)$ rises in the velocity interval $(0, v_{\rm AI})$. Vice versa, slow diffusion ($G < 1$) leads to negative $\partial f/\partial v$ and decrease of $f(v)$ in $(0, v_{\rm AI})$. Then, while v goes from $(0, v_{\rm AI})$ to $v > v_{\rm AI}$, AI manifests itself by the term $n_n^*\nu_{\rm AI}$ and the EVDF derivative becomes negative independent of the sign of $G - 1$ [see (7), (6)]. This means that the EVDF decreases at $v > v_{\rm AI}$ whether now $G > 1$ or $G < 1$. In accordance with the above, the qualitative behavior of $f(v)$ depends on the value of G (see Fig. 1). In the critical case of $G = 1$ the solution of Eq. (8) which satisfies the conditions $f(v = \infty) = 0$ and $f(v)$ bounded at the point $v = 0$ has the form

$$f^{\rm AI}(v) = \frac{2}{\pi} n_n^*\nu_{\rm AI} l_e \delta^{-1} v_0^{-4}\left\{\int_{v_{\rm AI}}^\infty \exp\left[-\frac{v^4 - v_{\rm AI}^4}{v_0^4}\right]\frac{dv}{v} - \theta(v - v_{\rm AI})\int_{v_{\rm AI}}^v \exp\left[-\frac{v'^4 - v_{\rm AI}^4}{v_0^4}\right]\frac{dv'}{v'}\right\}. \quad (9)$$

Relation (6) can be checked by the direct substitution of (9) to the left hand side of (6). The function $f^{\rm AI}(v)$ is shown in Fig. 1(c).

The EVDF is the Druyvesteyn function [10]

$$f^D(v) = \frac{n_e v_0^{-3}}{\pi\Gamma(3/4)} \exp\left[-\frac{v^4}{v_0^4}\right], \tag{10}$$

if one neglects electron diffusion and the energetic structure of the AI source in Eq. (7). Here n_e is the electron density and $\Gamma(u) = \int_0^\infty e^{-x}x^{u-1}dx$ the Euler gamma function. The Druyvesteyn function $f^D(v)$ gives the following mean electron energy:

$$\bar{\epsilon}^D = \frac{\Gamma(5/4)}{\Gamma(3/4)}\frac{mv_0^2}{2} = \frac{\Gamma(5/4)}{\Gamma(3/4)}\left(\frac{2e^2E^2l_e^2}{3\delta^{\rm el}}\right)^{1/2}. \tag{11}$$

In accordance with the above, just the calculations by formula (11) with an accurately known electric field E give a large systematic overestimation of $\bar{\epsilon}$, compared to the one obtained from the EVDF of Thomson scattering measurements. In contrast to this, the EVDF $f^{\rm AI}(v)$ gives the mean electron energy

$$\bar{\epsilon}^{\rm AI} = F(s)\frac{3}{5}\frac{mv_{\rm AI}^2}{2} = F(s)\tfrac{3}{5}\epsilon_{\rm AI}, \tag{12}$$

where

$$F(s) = \frac{\int_1^\infty x^4\exp(-sx^4)dx}{\int_1^\infty x^2\exp(-sx^4)dx}$$

and $s = (v_{\rm AI}/v_0)^4$. Figure 2 presents the dependence of the ratio

$$\frac{\bar{\epsilon}^{\rm AI}}{\bar{\epsilon}^D} = \frac{3}{5}\frac{\Gamma(3/4)}{\Gamma(5/4)}F(s)\sqrt{s} \tag{13}$$

on the parameter s. In experiment [5] $s \ll 1$. If s tends to zero, $F(s)\sqrt{s}$ tends to $\Gamma(5/4)/\Gamma(3/4)$. Thus the mean electron energy $\bar{\epsilon}^{\rm AI}$ obtained with the EVDF $f^{\rm AI}(v)$ (9) remains less ($5/3 \approx 1.67$ times) than the mean electron energy $\bar{\epsilon}^D$ obtained with the Druyvesteyn function $f^D(v)$ (10), even if the energy $mv_0^2/2$ goes to infinity.

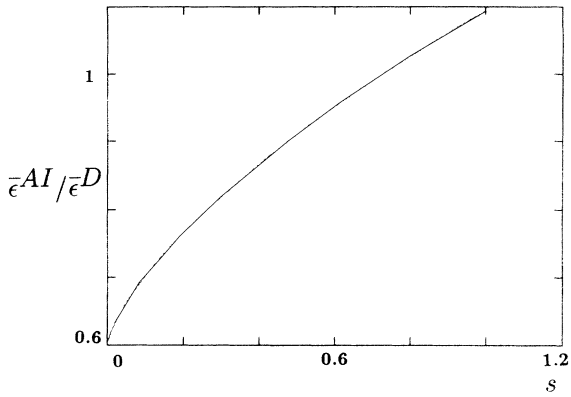

FIG. 2. The ratio between electron mean energies $\bar{\epsilon}^{\rm AI}$ and $\bar{\epsilon}^D$ obtained with distribution functions $f^{\rm AI}(v)$ (9) and $f^D(v)$ (10), respectively, as a function of $s = (v_{\rm AI}/v_0)^4 = [\epsilon_{\rm AI}/(mv_0^2/2)]^2$. Here $G = 1$.

Thus, accounting both for spatial electron diffusion and the energetic structure of the AI source leads to a mean electron energy which is smaller compared to that obtained by ignoring these factors.

Aiming at the comparison with experiment [5], one must take into account that the parameter $G \neq 1$. Indeed, for the conditions mentioned in [5], i.e., pressure $p = 2.26$ Torr and gas discharge glass tube radius $R = 1.1$ cm, one has $l_e = 2\times10^{-2}$ cm and $G = 1.1$. The last value is obtained with the assumption $a_0 = 2.405$, i.e., excluding for now the observed difference between the measured electron density profile $n_e(r)$ [20] and the Bessel function. The solution of Eq. (7) which satisfies the above two conditions $f(v=\infty) = 0$ and $f(v)$ bounded at the point $v = 0$ has the following form for arbitrary magnitude of the parameter G:

$$f^{\rm AI}(v) = \frac{1}{2\pi}n_n^*\nu_{\rm AI}l_e(\delta^{\rm el})^{-1}v_0^{-4}\exp\left[-\left(\frac{v}{v_0}\right)^4\right]\begin{cases}\Gamma(G)U(G,1,s)M\left(G,1,\left(\frac{v}{v_0}\right)^4\right) & \text{if } 0 \le v \le v_{\rm AI},\\ M(G,1,s)\Gamma(G)U\left(G,1,\left(\frac{v}{v_0}\right)^4\right) & \text{if } v > v_{\rm AI},\end{cases} \tag{14}$$

where $U(a,b,x)$ and $M(a,b,x)$ are the confluent hypergeometric functions [23]. For the experimental parameters $p = 2.26$ Torr, $R = 1.1$ cm, $E/p = 1.7$ V cm^{-1} Torr^{-1} [5], and $\epsilon_{\rm AI} = 0.68$ eV one has $mv_0^2/2 = 3.68$ eV, $s = 0.034$, and $G = 1.08$ at $a_0 = 2.405$. At these values the EVDF (14) leads to the mean electron energy $\bar{\epsilon}^{\rm AI}(G = 1.08) = 1.7$ eV, which is appreciably closer to the experimental one $\bar{\epsilon}^{\rm expt} = 1.3$ eV than $\bar{\epsilon}^D = 2.7$ eV, calculated with the help of the Druyvesteyn function (10).

Further, we will take into account that in accordance with experiment [20] one has to expect a more abrupt decrease of the electron density as a function of the distance r from the positive column axis. This means that the value a_0 must be increased in calculations compared to the magnitude of 2.405. This increase could be estimated as a factor of $\sqrt{2.5}$, since the increase of a_0^2 is about 2.5 [20]. This leads to the increase of G from $G = 1.08$ to $G = 2.7$. The EVDF (15) at the latter magnitude of G is represented in Fig. 1(a). This EVDF determines the mean electron energy of $\bar{\epsilon}^{\rm AI}(G = 2.7) = 1.3$ eV, which is in the best agreement with the experimental value [5].

It should be noted that in accordance with formula (14) the absolute value of the EVDF is determined by the density of excited atoms suitable for AI. This density is not determined in the above theory and thus the electron density appears to be a free parameter as in the Druyvesteyn theory [24] and many others (see, for example, [10]). Nevertheless, in addition to the above mean electron energy $\bar{\epsilon}^{\rm AI}$, the formula (14) enables one to carry

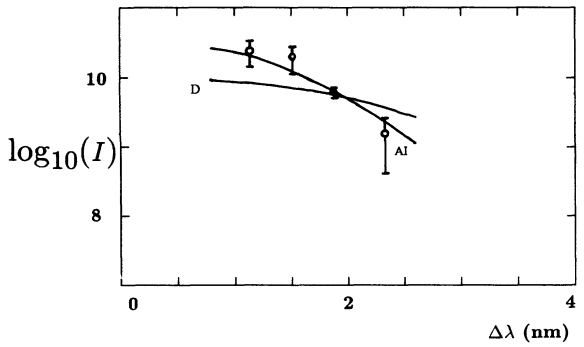

FIG. 3. Logarithm of Thomson scattering light intensities $\log_{10}[I^{\mathrm{AI}}(\Delta\lambda)]$ and $\log_{10}[I^{D}(\Delta\lambda)]$ as functions of scattered light wavelength shift $\Delta\lambda$, obtained from (15) with $f(v) = f^{\mathrm{AI}}(v)$ (curve AI), $f(v) = f^{D}(v)$ (curve D), respectively, and error bars of $\log_{10}(\Delta n_e/\Delta\lambda)$ [5] at $p = 2.26$ Torr, $R = 1.1$ cm, $E/p = 1.7$ V cm^{-1} Torr^{-1}, and $\epsilon_{\mathrm{AI}} = 0.68$ eV, which correspond to $s = 0.034$ and $G = 2.7$.

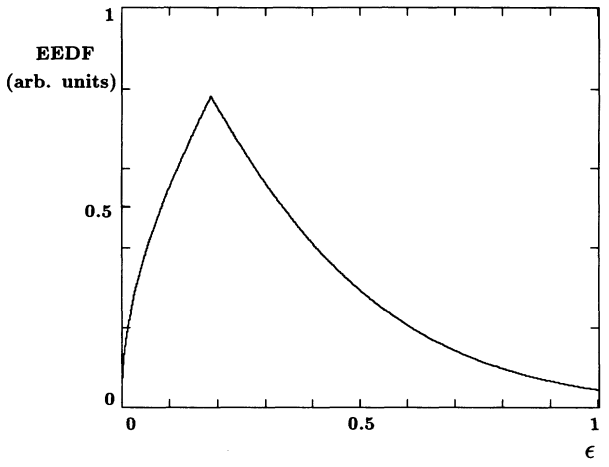

FIG. 4. EEDF in arbitrary units, which corresponds to the EVDF $f^{\mathrm{AI}}(v)$ (14) at $G = 2.7$ and $s = 0.034$, as a function of electron energy ϵ in units of the energy $mv_0^2/2$.

out a much better comparison with experiment [5]. Indeed, the Thomson light scattering intensity $I(\Delta\lambda)$ is proportional to the integral of $f(v)$,

$$I(\Delta\lambda) \sim \int_{V(\Delta\lambda)}^{\infty} f(v) v dv, \tag{15}$$

where $V(\Delta\lambda) = \Delta\lambda c/[2\lambda_0 \sin(\theta/2)]$, $\Delta\lambda$ is the Thomson scattering wavelength shift, λ_0 the wavelength of the probe laser beam, c the speed of light, and θ the angle between incident and scattered laser waves [25]. The last was equal to 90^0 in [5]. So by getting the integral of $f^{\mathrm{AI}}(v)$ in accordance with formula (15) one can compare the result $I^{\mathrm{AI}}(\Delta\lambda)$ with the experimental function $\Delta n_e/\Delta\lambda$ [5], implying the equality of electron densities $4\pi \int_0^{\infty} f^{\mathrm{AI}}(v) v^2 dv$ and the measured one [5]. Figure 3 presents $I^{\mathrm{AI}}(\Delta\lambda)$ at $p = 2.26$ Torr, $R = 1.1$ cm, $G = 2.7$, $E/p = 1.7$ V cm^{-1} Torr^{-1}, $s = 0.034$, and the error bars of [5]. Besides, Fig. 3 represents $I^{D}(\Delta\lambda)$ which is obtained from (15) with the Druyvesteyn function (10) at the parameters mentioned above. It is obvious from the figure that the theoretical curve $I^{\mathrm{AI}}(\Delta\lambda)$ is in fine agreement with the experimental bars, in contrast to $I^{D}(\Delta\lambda)$.

CONCLUSIONS

Thus, the EVDF measurements [5] at low electron densities of 10^{10} cm^{-3} with helium gas pressures about several Torr are in striking contradiction with the conventional point of view when a comparatively small mean electron energy leads to the Druyvesteyn EVDF [10,24]. Apart from this, taking into consideration the natural circumstances of spatial electron diffusion and energetic structure of the electron source, the theory of the present paper is in fine agreement with experiment, not only in the average characteristics such as mean electron energy but even in the functional behavior of scattered light (see Fig. 3).

The derived distribution function (14) demonstrates the peculiarity in the point $v = v_{\mathrm{AI}}$ (see Fig. 1), where $v_{\mathrm{AI}} = \sqrt{2\epsilon_{\mathrm{AI}}/m}$ is the velocity of electrons ejected during the AI with kinetic energy ϵ_{AI}. The last is strongly determined by the difference $\epsilon_{\mathrm{AI}} = \epsilon_{\mathrm{bi}} - \epsilon_{\mathrm{BE}}$ between the molecular ion binding energy ϵ_{bi} and the electron binding energy ϵ_{BE} in the excited helium atom He* [see reaction (1)]. The peculiarity mentioned above could be observed in experiment. Unfortunately, at the present time, the most popular are measurements of the electron energy distribution function (EEDF) (see, for example, [26]), which differs from the EVDF by the additional factor $\sqrt{\epsilon}$. Just the appearance of this factor makes observations of the peculiarity at $\epsilon = \epsilon_{\mathrm{AI}}$ difficult (see Fig. 4), because this factor introduces a comparatively sharp behavior of the EEDF in the interval $(0, \bar{\epsilon})$ and ϵ_{AI} just falls into this range. The appropriate algorithm to determine the EVDF from Langmuir–probe and Thomson scattering measurements was developed in [11]. It enables one to extract the EVDF from experimental noisy data.

ACKNOWLEDGMENTS

The author wishes to express his appreciation of the Arbeitsgruppe für Laser- und Plasmaphysik, Ruhr-Universität, 44780 Bochum, Federal Republic of Germany for cooperation.

[1] J. Benford, in *Proceedings of the International Conference on Phenomena in Ionized Gases XXI, 1993, Germany,* edited by G. Ecker, U. Arendt, and J. Böseler (APP, Bochum, 1993), Vol. 2, p. 116.

[2] F. Miethke, A. Rutscher, and H.-E. Wagner, in *Proceedings of the International Conference on Phenomena in Ionized Gases XXI, 1993, Germany* (Ref. [1]), Vol. 2, p. 205.

[3] H.-J. Tiller, F.-W. Breitbarth, D. Berg, and R. Kriegel, in *Proceedings of the International Conference on Phenomena in Ionized Gases XXI, 1993, Germany* (Ref. [1]), Vol. 2, p. 126.
[4] L. L. Alves, G. Gousset, and C. M. Ferreira, J. Phys. D **25**, 1713 (1992).
[5] H. J. Wesseling and B. Kronast, in *Proceedings of the International Conference on Phenomena in Ionized Gases XXI, 1993, Germany* (Ref. [1]), Vol. 2, p. 395. Error bars on Fig. 3 are reproduced from Fig. 2 of the above experimental work with kind permission. All additional data and information about the above experiment are private communications from H. J. Wesseling.
[6] R. P. Madden and K. Codling, Astrophys. J. **141**, 364 (1965).
[7] D. Barbiere, Phys. Rev. **84**, 653 (1951).
[8] J. A. Hornbeck and J. P. Molnar, Phys. Rev. **84**, 621 (1951).
[9] A. Hitachi, C. Davies, T. A. King, S. Kubota, and T. Doke, Phys. Rev. A **22**, 856 (1980).
[10] I. P. Schkarofsky, T. W. Johnston, and M. P. Bachynsky, *The Particle Kinetics of Plasmas* (Addison-Wesley, Reading, MA, 1965).
[11] M. V. Chegotov, J. Phys. D **27**, 54 (1994).
[12] P. L. Pakhomov and I. J. Fugol, Dokl. Akad. Nauk SSSR **159**, 57 (1964) [Sov. Phys. Dokl. **9**, 975 (1965)].
[13] C. B. Collins and W. W. Robertson, J. Chem. Phys. **40**, 2202; **40**, 2208 (1964).
[14] C. L. Chen, C. C. Leiby, and L. Goldstein, Phys. Rev. **121**, 391 (1961).
[15] H. J. Oskam and V. R. Mittelstadt, Phys. Rev. **132**, 1445 (1963).
[16] A. V. Phelps and S. C. Brown, Phys. Rev. **86**, 102 (1952).
[17] M. V. Chegotov, Kratk. Soobshch. Fiz. NN 3,4, 34 (1993) [Sov. Phys. Lebedev Inst. Rep. No. 4, 1 (1993)].
[18] M. V. Chegotov, Phys. Scr. **48**, 467 (1993).
[19] G. G. Lister, J. Phys. D **25**, 1649 (1992).
[20] M. Dietrich, S. Pfau, J. Rohmann, and H. Sievers, Verh. Dtsch. Phys. Ges. VI **28**, 127 (1993).
[21] H. S. W. Massey, E. H. S. Burhop, and H. B. Gilbody, *Electronic and Ionic Impact Phenomena*, 2nd ed. (Clarendon Oxford, 1974), Vol 4.
[22] S. A. Self and H. N. Ewald, Phys. Fluids **9**, 2486 (1966).
[23] *Handbook of Mathematical Functions*, edited by M. Abramowitz and I. A. Stegun (Dover, New York, 1964).
[24] M. J. Druyvesteyn, Physica **3**, 65 (1936).
[25] G. Bekefi, *Radiation Processes in Plasmas* (Wiley, New York, 1966).
[26] V. A. Godyak, R. B. Piejak, and B. M. Alexandrovich, Plasma Sources Sci. Technol. **1**, 36 (1992).